Signature of long-ranged spin triplets across a two-dimensional superconductor/helimagnet van der Waals interface

A. Spuri,[1] D. Nikolić [●],[1,2] S. Chakraborty [●],[1] M. Klang,[3] H. Alpern,[3] O. Millo,[3] H. Steinberg,[3] W. Belzig [●],[1]
E. Scheer,[1] and A. Di Bernardo [●][1,4,*]

[1]*Department of Physics, University of Konstanz, 78457 Konstanz, Germany*
[2]*Institut für Physik, Universität Greifswald, Felix-Hausdorff-Strasse 6, 17849 Greifswald, Germany*
[3]*Racah Institute of Physics, The Hebrew University of Jerusalem, 91904 Jerusalem, Israel*
[4]*Dipartimento di Fisica "E. R. Caianiello," Università degli Studi di Salerno, I-84084 Fisciano (SA), Italy*

The combination of a superconductor with a magnetically inhomogeneous material has been established as an efficient mechanism for the generation of long-ranged spin-polarized (spin-triplet) Cooper pairs. Evidence for this mechanism, however, has been demonstrated based on studies done on thin-film multilayers, where the strong bonds existing at the interface between the superconductor and the magnetic material should in principle enhance proximity effects and strengthen any electronic correlations. Here, we fabricate devices based on van der Waals (vdW) stacks of flakes of the NbS_2 combined with flakes of $Cr_{1/3}NbS_2$, which has a built-in magnetic inhomogeneity due to its helimagnetic spin texture at low temperatures. We find that the critical temperature of these vdW heterostructures is strongly dependent on the magnetic state of $Cr_{1/3}NbS_2$, whose degree of magnetic inhomogeneity can be controlled via an applied magnetic field. Our results demonstrate evidence for the generation of long-ranged spin-triplet pairs across the $Cr_{1/3}NbS_2/NbS_2$ vdW interface.

Introduction. The interplay between ferromagnetism and superconductivity has been widely investigated in superconductor/ferromagnet (S/F) thin-film multilayers with a conventional S, where the Cooper pairs of electrons are in an antiparallel-aligned (spin-singlet) state. Although early studies on such S/F hybrids showed that the magnetic exchange field (h_{ex}) of a F quickly suppresses the spin-singlet superconductivity from the S/F interface [1–3], over the past 20 years several groups have demonstrated, confirming a theoretical prediction [4], that long-ranged parallel-aligned (spin-triplet) Cooper pairs of electrons can be generated in S/F devices with noncollinear F's [5–9] or with an intrinsically inhomogeneous magnetic material like the helimagnet Ho [10–12]. Evidence for long-ranged spin triplets in these S/F hybrids has been found via measurements of the dependence of their superconducting critical temperature (T_c) on the magnetic state (i.e., collinear/noncollinear) [7–9] or via measurements of a long-ranged supercurrent (compared to the F's coherence length, ξ_F, for spin-singlet pairs) in S/F/S Josephson junctions (JJs) [4–6,10,13]. Spectroscopic evidence for spin-triplet states has also been reported via measurements of subgap states in the superconducting density of states [12,14,15] or via measurements of an inverse Meissner effect [11]. All these studies

have established the research field of superconducting spintronics [16] that aims at exploiting long-ranged spin triplets, which carry a net spin, to do spintronics in the superconducting state with low-energy dissipation.

Van der Waals (vdW) materials can be exfoliated down to the two-dimensional limit and exhibit physical properties that often do not have a counterpart in three-dimensional systems. Over the past years, a variety of vdW Ss and Fs have been explored both as single flakes and stacked to form vdW heterostructures [17–21]. S/F vdW heterostructures can be used to realize superconducting spintronic devices with novel functionalities compared to those based on thin-film multilayers. Before this occurs, however, it is essential to determine at which S/F vdW interfaces long-ranged spin triplets can be generated.

Several groups have recently studied the proximity effect in S/F vdW hybrids, and they have observed signatures of phenomena such as a 0-to-π transition in S/F/S vdW JJs [22], which had only been known for JJs made from thin-film multilayers [2,3]. Spin-triplet generation at the interface between electrodes of NbN (S) and the vdW material $Fe_{0.29}TaS_2$ (F) has also been reported [23], although this S/F interface may not be truly vdW in nature. A long-ranged coupling has also been measured in lateral $NbSe_2/Fe_3GeTe_2/NbSe_2$ (S/F/S) vdW JJs [24], but the spin-triplet nature of the supercurrent and the mechanism behind its generation remains unclear because Fe_3GeTe_2 does not have an intrinsic magnetic inhomogeneity.

In this Letter, we explore the superconducting proximity effect across the vdW interface forming between a flake of a vdW S (NbS_2) and a magnetic flake of $Cr_{1/3}NbS_2$. $Cr_{1/3}NbS_2$

---

*Corresponding author: angelo.dibernardo@uni-konstanz.de
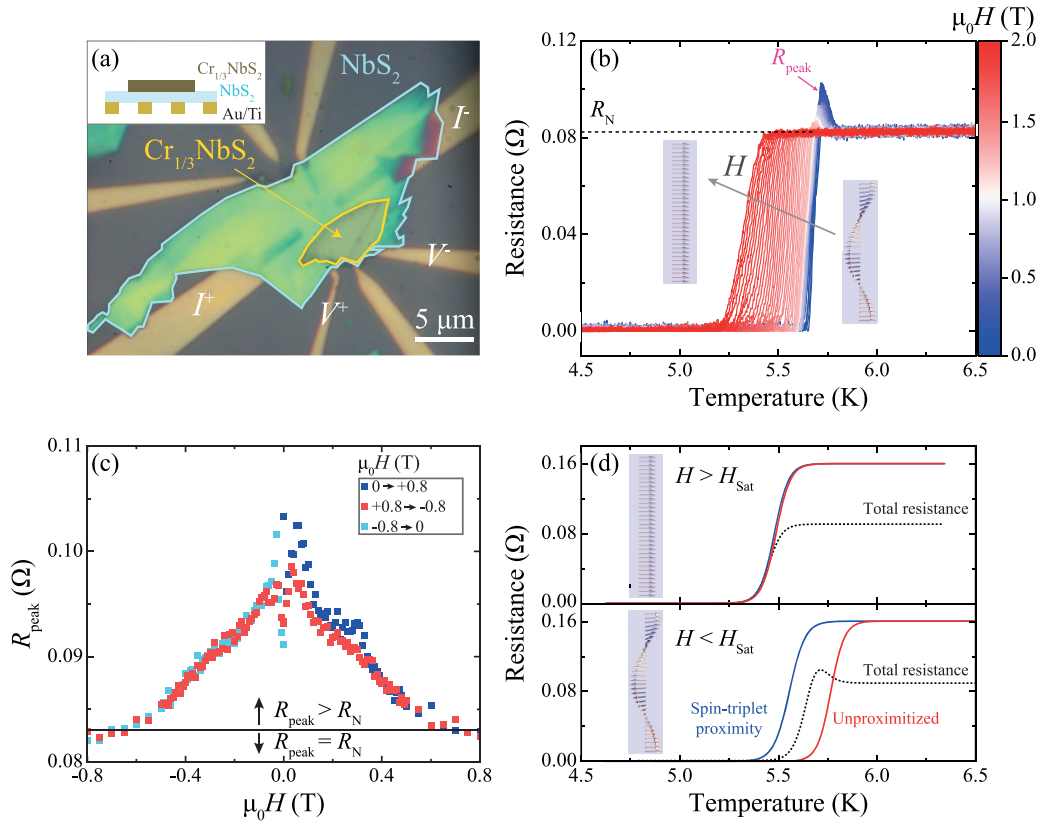
FIG. 1. (a) Optical microscope image of a $Cr_{1/3}NbS_2$ (200 nm)/NbS_2 (20 nm) vdW heterostructure on Au (23 nm)/Ti (7 nm) electrodes, with the inset showing the materials stack, and corresponding $R(T)$ as a function of an in-plane H in (b). The R_{peak} feature vanishes as H is increased above H_{sat}. (c) R_{peak} versus H for H ranges specified in the legend. (d) Model showing the origin of R_{peak} due to the presence of regions with different T_c for $H < H_{sat}$ (bottom panel) assuming equal T_c for $H > H_{sat}$ (top panel). Red and blue curves refer to bare NbS_2 and $Cr_{1/3}NbS_2/NbS_2$, respectively.

is helimagnetic at low temperatures [25,26] and therefore has a built-in magnetic inhomogeneity ideal for spin-triplet generation. Studying the evolution of the T_c of $Cr_{1/3}NbS_2/NbS_2$ (F/S) stacks as a function of the magnetic state of $Cr_{1/3}NbS_2$, we find that the T_c of these vdW devices strongly depends on the $Cr_{1/3}NbS_2$ magnetization, in a way that cannot be reconciled with a conventional short-ranged S/F proximity effect or with stray fields. Supported also by a theoretical model, we show that our results are consistent with the generation of long-ranged spin-triplet pairs across the $Cr_{1/3}NbS_2/NbS_2$ vdW interface.

Results and discussion. We fabricate vdW heterostructures of $Cr_{1/3}NbS_2/NbS_2$ ($Cr_{1/3}NbS_2$ on top) on prepatterned Au(33 nm)/Ti(7 nm) electrodes using the dry-transfer technique [27], as shown in Fig. 1(a). We use $Cr_{1/3}NbS_2$ flakes with thickness ranging between 200 and 500 nm, which are obtained via subsequent mechanical cleaving and exfoliation of $Cr_{1/3}NbS_2$ single crystals synthesized as in Ref. [25].

We choose $Cr_{1/3}NbS_2$ as our magnetic flake because it is the closest equivalent to the helimagnet Ho, which previous studies on S/F thin-film multilayers have shown to be efficient for spin-triplet generation [10–12]. Like in Ho, the helimagnetic spin texture of $Cr_{1/3}NbS_2$ can be unzipped by an in-plane magnetic field H which, above a certain value depending on thickness [25,26], makes $Cr_{1/3}NbS_2$ fully ferromagnetic. This property provides a tool to control whether any observed ef-

fects are due to long-ranged spin triplets because such triplets should be only generated in the magnetically inhomogeneous (helimagnetic) state of $Cr_{1/3}NbS_2$ and be suppressed when $Cr_{1/3}NbS_2$ is driven into its magnetically homogeneous (ferromagnetic) state.

$Cr_{1/3}NbS_2$ is an ionic compound, which makes it difficult to obtain flakes with thickness smaller than 50 nm [25,26]. Nonetheless, this is not a limitation for our experiment, since we deliberately chose $Cr_{1/3}NbS_2$ flakes with thickness larger than 200 nm. Thick flakes of $Cr_{1/3}NbS_2$ are necessary because, if long-ranged spin-triplet pairs are generated at the $Cr_{1/3}NbS_2/NbS_2$ vdW interface, these pairs must have enough room to propagate into $Cr_{1/3}NbS_2$ for them to affect the T_c of the proximitized NbS_2. Theory and experiments on S/F thin-film multilayers have in fact shown that, to maximize the effect of long-ranged spin triplets on T_c, a F with thickness d_F larger than its ξ_F is needed [9,28]. To increase the effect on T_c, the S should also have thickness d_S comparable to or smaller than its superconducting coherence length (ξ_S) [8,9].

The reason why long-ranged spin triplets can reduce the T_c of a S/F heterostructure with $d_S \sim \xi_S$ and $d_F > \xi_F$ can be understood by thinking of a S as a reservoir of Cooper pairs: once long-ranged spin-triplet pairs are generated, they can propagate deeply into the F (much deeper than ξ_F), which drains pairs out of the S and reduces T_c. On the other hand, if only short-ranged spin-triplet pairs are generated, the

proximity effect remains confined at the S/F interface within ξ_F (typically a few nanometers [29]) and T_c is higher.

To determine whether long-ranged spin triplets are generated in our $Cr_{1/3}NbS_2/NbS_2$ devices, we study the evolution of their resistance versus temperature, $R(T)$, measured across T_c, as a function of an in-plane H (i.e., perpendicular to the $Cr_{1/3}NbS_2$ c axis). As H is increased, the helimagnetic texture of $Cr_{1/3}NbS_2$ progressively unzips until H reaches a saturation field (H_{sat}), at which $Cr_{1/3}NbS_2$ becomes ferromagnetic [25,26].

For the $Cr_{1/3}NbS_2/NbS_2$ device in Fig. 1(a), the $R(T)$ curve measured in $H = 0$ shows a peaklike feature, R_{peak}, at the onset of the superconducting transition. R_{peak} persists in the helimagnetic state of $Cr_{1/3}NbS_2$ as H is increased and it vanishes as H approaches $\mu_0 H_{sat} \sim 0.5$ T (μ_0 being the vacuum permeability). At $H > H_{sat}$, R_{peak} coincides with the normal-state resistance of the device (R_N) at $T \sim 6.0$ K [Figs. 1(b) and 1(c)]. These observations and the fact that R_{peak} is only measured in this device with a specific arrangement of contacts rule out magnetic impurities as an explanation for R_{peak}. The data reported in Fig. 1(c) also show that, as the H polarity is reversed and H is decreased below H_{sat}, R_{peak} reappears in the helimagnetic state of $Cr_{1/3}NbS_2$ before vanishing again at $H \sim -H_{sat}$. These results suggest that R_{peak} must be correlated to the magnetically inhomogeneous state of $Cr_{1/3}NbS_2$.

To understand the R_{peak} origin, we note that, for the device in Fig. 1(a), we inject the current with two electrodes (I^- and I^+) that are contacting only the bare NbS_2, and we collect the voltage signal with two other electrodes (V^- and V^+) placed under the $Cr_{1/3}NbS_2/NbS_2$ stack. These two regions (i.e., bare NbS_2 and $Cr_{1/3}NbS_2/NbS_2$ stack) may have different T_c, which should be lower for the S/F stack due to the proximity effect [29]. As done in Ref. [30], where a similar R_{peak} is observed, in the Supplemental Material [31] we show that R_{peak} can be reproduced considering a network of resistors equivalent to our sample, where each resistor corresponds to a sample region with different T_c. Our analysis also confirms that the regions in the F/S stack have a lower T_c than those in the bare S.

For R_{peak} to vanish at $|H| > H_{sat}$, the T_c of the F/S stack ($T_{c,bi}$), which is lower than the T_c of the bare S ($T_{c,bare}$) for $H < H_{sat}$, must become closer to $T_{c,bare}$ when $H > H_{sat}$ [Fig. 1(d)]. This behavior of $T_{c,bi}$ is opposite to that expected for a F/S proximity with a homogeneous F or for stray fields, since both effects should get stronger and decrease $T_{c,bi}$ as $Cr_{1/3}NbS_2$ is driven ferromagnetic (see discussion below).

The positive shift of $T_{c,bi}$ towards $T_{c,bare}$ for $H > H_{sat}$ [Fig. 1(d)], which leads to the R_{peak} disappearance, can be due to an unconventional proximity effect at the $Cr_{1/3}NbS_2/NbS_2$ (F/S) vdW interface involving long-ranged spin triplets. This is because, when $Cr_{1/3}NbS_2$ is in its helimagnetic state, long-ranged spin triplets can be generated and can propagate deeply into $Cr_{1/3}NbS_2$ reducing $T_{c,bi}$ compared to $T_{c,bare}$ [Fig. 1(d); bottom]. As $Cr_{1/3}NbS_2$ is driven ferromagnetic for $H > H_{sat}$, only short-ranged Cooper pairs can be generated, which remain confined close to the $Cr_{1/3}NbS_2/NbS_2$ interface making $T_{c,bi}$ approach $T_{c,bare}$ [Fig. 1(d); top].

The F/S vdW device in Fig. 1, however, makes it difficult to argue generation of long-ranged spin triplets across

the $Cr_{1/3}NbS_2/NbS_2$ vdW interface due the presence of two contributions (from bare NbS_2 and $Cr_{1/3}NbS_2/NbS_2$ stack) to the total $R(T)$.

To validate our interpretation of the data in Fig. 1, we make another $Cr_{1/3}NbS_2/NbS_2$ vdW device [Fig. 2(a)], where all electrodes are in contact with the $Cr_{1/3}NbS_2/NbS_2$ stack. As shown in Fig. 2(b), the $R(T)$ of this device does not exhibit any R_{peak}, independently on H, which supports our claim that R_{peak} in Fig. 1 originates from two regions with different T_c.

To determine if long-ranged spin triplets affect the $T_{c,bi}$ of the device in Fig. 2(a), from each of the $R(T)$ curves in Fig. 2(b), we extract $T_{c,bi}$ defined as the T where R reaches 50% of its normal-state value at $T = 6.0$ K ($T_c \sim 5.75$ K). Based on these $T_{c,bi}$ values, we study how $T_{c,bi}$ varies with H, $T_{c,bi}(H)$, for both increasing and decreasing H [Fig. 3(a)]. We always apply H in the normal state of our devices at $T = 7.0$ K and, at every H, we record $R(T)$ while both cooling (from 7.0 down to 3.0 K) and warming (from 3.0 to 7.0 K) our samples, to extract the corresponding $T_{c,bi}$ values. Unless differently specified, the $T_{c,bi}(H)$ curves shown are based on sample-cooling $T_{c,bi}$ data.

$T_{c,bi}(H)$ for the device in Fig. 2(a) is shown in Fig. 3(a), for both H upsweep (blue curve) and downsweep (red curve). As H is increased, $T_{c,bi}(H)$ shows a first feature (at $\mu_0 H < 60$ mT) followed by a decrease with different slope at 60 mT $< \mu_0 H < \mu_0 H_{sat}$ and then by a positive shift at $H = H_{sat}$. During the H downsweep, for $H > H_{sat}$, $T_{c,bi}(H)$ coincides with $T_{c,bi}(H)$ measured during the H upsweep, but shows a difference of ~ 20 mK from the latter for $H < H_{sat}$.

The positive shift in $T_{c,bi}(H)$ at $H \sim H_{sat}$ in Fig. 3(a) is consistent with our explanation for the data in Fig. 1 and the disappearance of R_{peak} at $H \sim H_{sat}$ due to a positive $T_{c,bi}$ shift. Also for this device in Fig. 3(a), if long-ranged spin triplets are generated, then $T_{c,bi}(H)$ in the $Cr_{1/3}NbS_2$ helimagnetic state ($H < H_{sat}$) must be lower than $T_{c,bi}(H)$ in the $Cr_{1/3}NbS_2$ ferromagnetic state ($H > H_{sat}$), meaning that $T_{c,bi}$ should exhibit a positive shift at $H \sim H_{sat}$, as we observe. Consistently with the disappearance of R_{peak} in Fig. 1(b), the jump in $T_{c,bi}(H)$ at $H \sim H_{sat}$ in Fig. 3(a) cannot be due to a conventional F/S proximity involving short-ranged Cooper pairs or due to stray fields, since both effects should decrease rather than increase $T_{c,bi}$ at $H \sim H_{sat}$. Vortices also cannot account for our results, as discussed in the Supplemental Material [31].

To rule out stray fields, like in previous studies on thin-film multilayers [15,32], we fabricate a vdW device where a 10-nm-thick insulator (I) of hexagonal boron nitride is placed between $Cr_{1/3}NbS_2$ and NbS_2 to suppress any superconducting proximity effects. The T_c profile of this F/I/S vdW heterostructure (Supplemental Material Fig. S4 [31]), $T_{c,tri}(H)$, shows some features at $\mu_0 H < 100$ mT like those in Fig. 3(a) for $\mu_0 H < 60$ mT, which we associate to stray fields, but then follows a parabolic trend different from $T_{c,bi}(H)$ in Fig. 3(a). This parabolic trend resembles that measured for bare NbS_2 (S) (Supplemental Fig. S5 [31]). Also, $T_{c,tri}(H)$ has a negative rather than a positive jump at $H \sim H_{sat}$, unlike $T_{c,bi}(H)$ in Fig. 3(a), confirming that stray fields should get stronger and reduce $T_{c,bi}$ at $H \sim H_{sat}$. Based on these results for the F/I/S device, we conclude that only the features in $T_{c,bi}(H)$ at $\mu_0 H < 60$ mT in Fig. 3(a) are due to stray fields, while all the other features, including the positive jump at
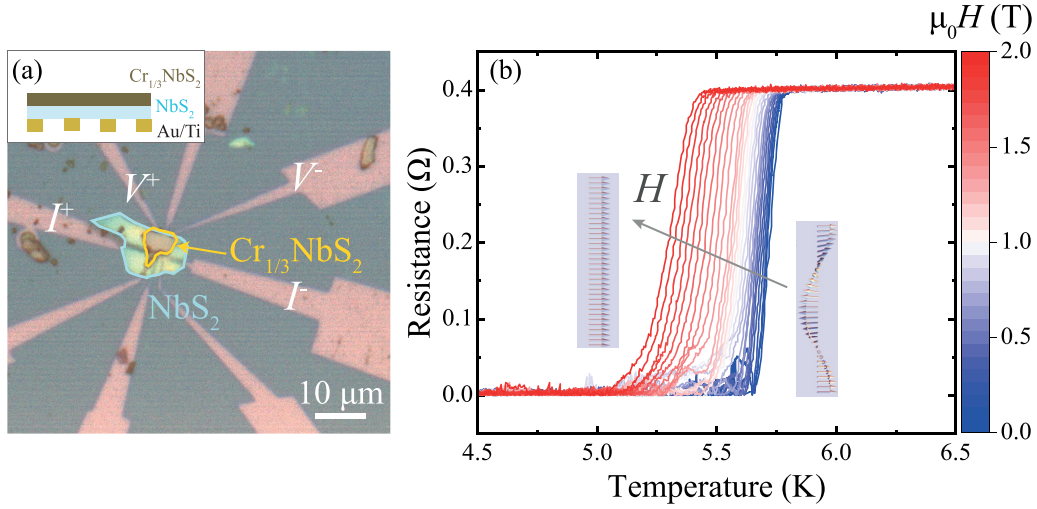
FIG. 2. (a) Optical microscope image of a $Cr_{1/3}NbS_2$ (350 nm)/NbS_2 (25 nm) vdW heterostructure made on Au (33 nm)/Ti (7 nm) electrodes with the inset showing the materials stack and corresponding $R(T)$ in (b) as a function of an in-plane H (values in the color bar) used to switch $Cr_{1/3}NbS_2$ from a helimagnetic to a ferromagnetic state.

$H \sim H_{sat}$, are due to a proximity effect involving long-ranged spin triplets.

Spectroscopic studies on Nb/Ho thin films have shown that spin-triplet generation is sensitive to the misalignment of the magnetic moments near the Nb/Ho interface, compared to the bulk Ho helix [12]. Like for Nb/Ho [12], interface magnetic moments misaligned to the $Cr_{1/3}NbS_2$ helix can have a non-null out-of-plane component and generate dipolar fields into NbS_2, which can account for the $T_{c,bi}(H)$ variation at low H in our S/F vdW devices.

Previous transport experiments on epitaxial Ho/Nb thin-film heterostructures [33] also show, consistently with our results, that $T_{c,bi}$ decreases as Ho is driven from its helimagnetic to ferromagnetic state by an in-plane H. However, when Ho becomes ferromagnetic, a negative shift in $T_{c,bi}$ is observed which, as argued by the authors, is opposite to that expected for spin-triplet generation. By contrast, in our F/S vdW devices, we observe a positive shift in $T_{c,bi}(H)$ at $H \sim H_{sat}$.

In addition to the F/S vdW device in Fig. 3(a), we have made another F/S vdW device with thinner NbS_2 ($\sim$10 nm), to determine whether the shift in $T_{c,bi}$ increases as d_S gets reduced and closer to ξ_S, which would further indicate that the $T_{c,bi}(H)$ shift is due to a superconducting proximity effect. As shown in Supplemental Material Fig. S5(a) [31], this device has two regions: one made of a $Cr_{1/3}NbS_2$/NbS_2 stack and the other made of bare NbS_2 (S) but of the same NbS_2 flake used for the F/S stack. Each of these regions has its own set of electrodes to measure $T_{c,bare}(H)$ independently on $T_{c,bi}(H)$. For this device, we find that $T_{c,bare}(H)$ has a parabolic trend consistent with H-induced orbital depairing [Supplemental Material Fig. S5(b) [31]]. In contrast, $T_{c,bi}(H)$ deviates from $T_{c,bare}(H)$ for $H < H_{sat}$ and shows a first drop

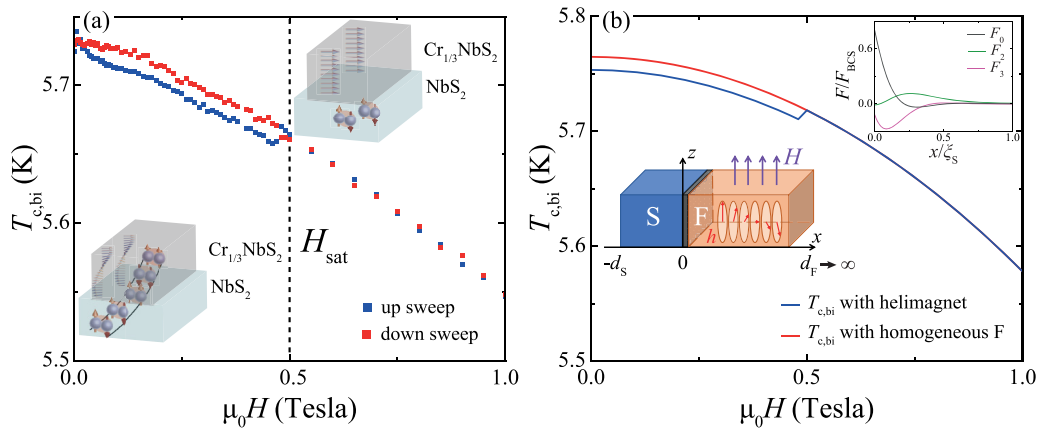FIG. 3. (a) T_c versus in-plane H of a $Cr_{1/3}NbS_2$/NbS_2 device, $T_{c,bi}(H)$, determined from $R(T)$ curves in Fig. 2(b) for H upsweep (blue curve) and downsweep (red curve). The lower and upper sketches show the magnetic configuration of $Cr_{1/3}NbS_2$ for $H < H_{sat}$ and $H > H_{sat}$, respectively. (b) Theoretical $T_{c,bi}(H)$ for a S/F with a helimagnet becoming ferromagnetic at H_{sat} (blue curve) and for S/F with a homogeneous ferromagnet (red curve). The theoretical model used is shown in the lower panel, while the upper inset shows the decay of pairing amplitudes from the S/F interface in the F helimagnetic state: spin singlets (F_0), long-ranged triplets (F_2), and short-ranged triplets (F_3).

at $\mu_0 H < 80$ mT, which we ascribe to stray fields, followed by a slower decrease that we relate to spin-triplet generation (see above). For $H > H_{sat}$, where long-ranged spin triplets cannot be generated, $T_{c,bi}(H)$ follows $T_{c,bare}(H)$, but with a constant (negative) offset due to h_{ex}. For 80 mT $< \mu_0 H < \mu_0 H_{sat}$, the proximity effect must therefore involve long-ranged spin triplets, since a F/S proximity with short-ranged triplets, which occurs for $H > H_{sat}$, gives a $T_{c,bi}(H)$ profile like $T_{c,bare}(H)$ (see theory model below). Also, the shift in $T_{c,bi}$ from $T_{c,bare}$ for this device is ~ 40 mK at $H < H_{sat}$, which is larger than that in Fig. 3(a), consistently with the decrease in NbS$_2$ thickness from 20 to 10 nm.

To support our claims that long-ranged spin triplets are generated at the Cr$_{1/3}$NbS$_2$/NbS$_2$ vdW interface, we develop a model describing the proximity effect in our F/S system. Our theoretical description of the effect is based on the quasiclassical Green's function method in the diffusive limit (Usadel approach). A sketch of our model is reported in the inset of Fig. 3(b). We consider a S of length d_S coupled to an infinitely long helimagnet F with $d_F \gg \xi_F$. The in-plane magnetization (in the $y - z$ plane) of the helimagnet is modeled using the exchange field $\boldsymbol{h}_{ex} = h_{ex}(\boldsymbol{e}_y \sin qx + \boldsymbol{e}_z \cos qx)$, where q relates to the pitch of the helix $(2\pi/q)$ defined along the x direction perpendicular to the S/F interface. The quality of the interface in our model is related to the parameter γ_B (see Supplemental Material [31]), which defines the interface transparency, and to $\gamma = \sigma_F/\sigma_S$ depending on the mismatch between the normal-state conductivities of F (σ_F) and S (σ_S). We assume that an in-plane H is applied (along the z direction), which modulates the F's magnetic textures and penetrates the S affecting $T_{c,bi}$, and we only consider H-induced orbital depairing. Also, we simply assume that the transition from a helimagnetic to a ferromagnetic state in F occurs abruptly at H_{sat} like for the device in Fig. 3(a) and we model it as a step function.

Our hypothesis is that an inhomogeneous (helical) magnetization in a F can generate long-range spin-triplet correlations at the S/F interface thus suppressing the superconducting gap in S. Effectively, this gap suppression is seen in our theoretical curves as a reduction of the superconducting critical temperature $T_{c,bi}$. We observe that the theoretical $T_{c,bi}(H)$ in Fig. 3(b) (blue curve) calculated with our model for a helimagnet becoming ferromagnetic at $\mu_0 H_{sat} \sim 0.5$ T is in very good agreement with the experimental data in Fig. 3(a). In the same Fig. 3(b), we also report the theoretical $T_{c,bi}(H)$ profile

(red curve) calculated for a S/F system with a homogeneous h_{ex} confirming a parabolic trend.

The inset of Fig. 3(b) shows the anomalous Green's functions (pairing amplitudes) as a function of the position x inside F. We find that the helical ordering of the F induces a nonvanishing long-ranged pairing amplitude, which suppresses the S gap and reduces $T_{c,bi}$. The curves in Fig. 3(b) are calculated using the following parameters: $d_S = 2\xi_S$, $\gamma = 0.055$, $\gamma_B = 0$, $q\xi_S = 3$, $h/\Delta_0 = 100$, $\xi_S = 10$ nm (Δ_0 being the NbS$_2$ superconducting gap). The bulk T_c and upper critical field of S are assumed to be $T_{c,S} = \Delta_0/(1.764\,k_B) = 6.3$ K (k_B being the Boltzmann constant) and $\mu_0 H_{c,S} = 5$ T, respectively. The only fitting parameters are γ and γ_B, whereas all the other parameters are taken from the literature or estimated. The best fits for $T_{c,bi}(H)$ are obtained for $\gamma_B = 0$, which suggests that the F/S vdW interface must have a good transparency, to observe our experimental results. This confirms that we can get a strong proximity effect in our devices despite the weak vdW nature of their F/S interfaces.

In conclusion, the dependence of $T_{c,bi}$ in Cr$_{1/3}$NbS$_2$/NbS$_2$ devices on the magnetic state of Cr$_{1/3}$NbS$_2$ is consistent with the generation of long-ranged spin-triplet pairs across their vdW interface. A strong proximity effect involving long-ranged spin-triplet pairs can therefore not only occur across a S/F interface with strong covalent bonds, as already reported, but also across a weakly bonded vdW interface. Our results pave the way for the combination of helimagnetic metals like Cr$_{1/3}$NbS$_2$ (or stacks of vdW ferromagnets) with other vdW superconductors to both realize devices recently proposed [34,35] and study how spin-triplet pairs can be generated and manipulated in vdW systems for superconducting spintronics.

[1] T. Kontos, M. Aprili, J. Lesueur, and X. Grison, Inhomogeneous superconductivity induced in a ferromagnet by proximity effect, Phys. Rev. Lett. **86**, 304 (2001).

[2] V. V. Ryazanov, V. A. Oboznov, A. Yu. Rusanov, A. V. Veretennikov, A. A. Golubov, and J. Aarts, Coupling of two superconductors through a ferromagnet: Evidence for a π junction, Phys. Rev. Lett. **86**, 2427 (2001).

[3] Y. Blum, A. Tsukernik, M. Karpovski, and A. Palevski, Oscillations of the superconducting critical current in Nb-Cu-Ni-Cu-Nb junctions, Phys. Rev. Lett. **89**, 187004 (2002).

[4] F. S. Bergeret, A. F. Volkov, and K. B. Efetov, Long-range proximity effects in superconductor-ferromagnet structures, Phys. Rev. Lett. **86**, 4096 (2001).

[5] T. S. Khaire, M. A. Khasawneh, W. P. Pratt, and N. O. Birge, Observation of spin-triplet superconductivity in Co-based Josephson junctions, Phys. Rev. Lett. **104**, 137002 (2010).

[6] C. Klose, T. S. Khaire, Y. Wang, W. P. Pratt Jr., N. O. Birge, B. J. McMorran, T. P. Ginley, J. A. Borchers, B. J. Kirby, B. B. Maranville, and J. Unguris, Optimization of spin-triplet

supercurrent in ferromagnetic Josephson junctions, Phys. Rev. Lett. **108**, 127002 (2012).

[7] P. V. Leksin, N. N. Garif'yanov, I. A. Garifullin, Ya. V. Fominov, J. Schumann, Y. Krupskaya, V. Kataev, O. G. Schmidt, and B. Büchner, Evidence for triplet superconductivity in a superconductor-ferromagnet spin valve, Phys. Rev. Lett. **109**, 057005 (2012).

[8] X. L. Wang, A. Di Bernardo, N. Banerjee, A. Wells, F. S. Bergeret, M. G. Blamire, and J. W. A. Robinson, Giant triplet proximity effect in superconducting pseudo spin valves with engineered anisotropy, Phys. Rev. B **89**, 140508(R) (2014).

[9] A. Singh, S. Voltan, K. Lahabi, and J. Aarts, Colossal proximity effect in a superconducting triplet spin valve based on the half-metallic ferromagnet CrO_2, Phys. Rev. X **5**, 021019 (2015).

[10] J. W. A. Robinson, J. D. S. Witt, and M. G. Blamire, Controlled injection of spin-triplet supercurrents into a strong ferromagnet, Science **329**, 59 (2010).

[11] A. Di Bernardo, Z. Salman, X. L. Wang, M. Amado, M. Egilmez, M. G. Flokstra, A. Suter, S. L. Lee, J. H. Zhao, T. Prokscha, E. Morenzoni, M. G. Blamire, J. Linder, and J. W. A. Robinson, Intrinsic paramagnetic Meissner effect due to *s*-wave odd-frequency superconductivity, Phys. Rev. X **5**, 041021 (2015).

[12] A. Di Bernardo, S. Diesch, Y. Gu, J. Linder, E. Scheer, M. G. Blamire, and J. W. A. Robinson, Signature of magnetic-dependent gapless odd frequency states at superconductor/ferromagnet interfaces, Nat. Commun. **6**, 8053 (2015).

[13] R. S. Keizer, S. T. B. Gonnenwein, T. M. Klapwijk, G. Miao, G. Xiao, and A. Gupta, A spin triplet supercurrent through the half-metallic ferromagnet CrO_2, Nature (London) **439**, 825 (2006).

[14] S. Diesch, P. Machon, M. Wolz, C. Sürgers, D. Beckmann, W. Belzig, and E. Scheer, Creation of equal-spin triplet superconductivity at the Al/EuS interface, Nat. Commun. **9**, 5248 (2018).

[15] Y. Kalcheim, O. Millo, A. Di Bernardo, A. Pal, and J. W. A. Robinson, Inverse proximity effect at superconductor-ferromagnet interfaces: Evidence for induced triplet pairing in the superconductor, Phys. Rev. B **92**, 060501(R) (2015).

[16] J. Linder and J. W. A. Robinson, Superconducting spintronics, Nat. Phys. **11**, 307 (2015).

[17] M. Gibertini, M. Koperski, A. F. Mopurgo, and K. S. Novoselov, Magnetic 2D materials and heterostructures, Nat. Nanotechnol. **14**, 408 (2019).

[18] M. C. Wang, C. C. Huang, C. H. Cheung, C. Y. Chen, S. G. Tan, T. W. Huang, Y. Zhao, Y. Zhao, G. Wu, Y. P. Feng, H. C. Wu, and C. R. Chang, Prospects and opportunities of 2D van der Waals magnetic systems, Ann. Phys. **532**, 1900452 (2020).

[19] X. Xi, Z. Wang, W. Zhao, J. H. Park, K. T. Law, H. Berger, L. Forró, J. Shan, and K. F. Mak, Ising pairing in superconducting NbSe2 atomic layers, Nat. Phys. **12**, 139 (2016).

[20] E. Navarro-Moratalla, J. O. Island, S. Mañas-Valero, E. Pinilla-Cienfuegos, A. Castellanos-Gomez, J. Quereda, G. Rubio-Bollinger, L. Chirolli, J. A. Silva-Guillen, N. Agraït, G. A. Steele, F. Guinea, H. S. J. van der Zant, and E. Coronado, Enhanced superconductivity in atomically thin TaS_2, Nat. Commun. **7**, 11043 (2016).

[21] R. Yan, G. Khalsa, B. T. Schaefer, A. Jarjour, S. Rouvimov, K. C. Nowack, H. G. Xing, and D. Jena, Thickness dependence of superconductivity in ultrathin NbS2, Appl. Phys. Express **12**, 023008 (2019).

[22] K. Kang, H. Berger, K. Watanabe, T. Taniguchi, L. Forró, J. Shan, and K. F. Mak, van der Waals π Josephson junctions, Nano Lett. **22**, 5510 (2022).

[23] R. Cai, Y. Yao, P. Lv, Y. Ma, W. Xing, B. Li, Y. Ji, H. Zhou, C. Shen, S. Jia, X. C. Xie, I. Zutic, Q. F. Sun, and W. Han, Evidence for anisotropic spin-triplet Andreev reflections at the 2D van der Waals ferromagnet/superconductor interface, Nat. Commun. **12**, 6725 (2021).

[24] G. Hu, C. Wang, S. Wang, Y. Zhang, Y. Feng, Z. Wang, Q. Niu, Z. Zhang, and B. Xiang, Long-range skin Josephson supercurrent across a van der Waals ferromagnet, Nat. Commun. **14**, 1779 (2023).

[25] S. Tang, R. S. Fishman, S. Okamoto, J. Yi, Q. Zou, M. Fu, A. P. Li, D. Mandrus, and Z. Gai, Tuning magnetic soliton phase via dimensional confinement in exfoliated 2D $Cr_{1/3}NbS_2$ thin flakes, Nano Lett. **18**, 4023 (2018).

[26] L. Wang, N. Chepiga, D. K. Ki, L. Li, F. Li, W. Zhu, Y. Kato, O. S. Ovchinnikova, F. Mila, I. Martin, D. Mandrus, and A. F. Mopurgo, Controlling the topological sector of magnetic solitons in exfoliated $Cr_{1/3}NbS_2$ crystals, Phys. Rev. Lett. **118**, 257203 (2017).

[27] S. Fan, Q. A. Vu, M. D. Tran, S. Adhikari, and Y. H. Lee, Transfer assembly for two-dimensional van der Waals heterostructures, 2D Mater. **7**, 022005 (2020).

[28] Ya. V. Fominov, A. A. Golubov, T. Yu. Karminskaya, M. Yu. Kupriyanov, R. G. Deminov, and L. R. Tagirov, Superconducting triplet spin valve, JETP Lett. **91**, 308 (2010).

[29] A. I. Buzdin, Proximity effects in superconductor-ferromagnet heterostructures, Rev. Mod. Phys. **77**, 935 (2005).

[30] R. Vaglio, C. Attanasio, L. Maritato, and A. Ruosi, Explanation of the resistance-peak anomaly in non-homogeneous superconductors, Phys. Rev. B **47**, 15302 (1993).

[31] See Supplemental Material at http://link.aps.org/supplemental/10.1103/PhysRevResearch.6.L012046 for the model of the resistance peak R_{peak} in Fig. 1; additional low-temperature magnetotransport data on other S/F vdW heterostructures and S/I/F vdW heterostructures (I being an insulator); and the model based on the quasiclassical Green's function method of the theoretical $T_c(H)$ profile in Fig. 3(b). The Supplemental Material also contains Refs. [4,26,30] of the main text.

[32] A. Stellhorn, A. Sarkar, E. Kentzinger, J. Barthel, A. Di Bernardo, S. Nandi, P. Zakalek, J. Schubert, and T. Brückel, Tailoring superconducting states in superconductor-ferromagnet hybrids, New J. Phys. **22**, 093001 (2020).

[33] Y. Gu, J. W. A. Robinson, M. Bianchetti, N. A. Stelmashenko, D. Astill, F. M. Grosche, J. L. MacManus-Driscoll, and M. G. Blamire, Magnetic state controllable critical temperature in epitaxial Ho/Nb bilayers, APL Mater. **2**, 046103 (2014).

[34] N. A. Gusev, D. I. Dgheparov, N. G. Pugach, and V. I. Belotelov, Magnonic control of the superconducting spin valve by magnetization reorientation in a helimagnet, Appl. Phys Lett. **118**, 232601 (2021).

[35] N. G. Pugach, D. M. Heim, D. V. Seleznev, A. I. Chernov, and D. Menzel, Switchable spiral Josephson junction: A superconducting spin-valve proposal, Supercond. Sci. Technol. **35**, 025002 (2022).